Computer Assisted Methods in Engineering and Science
31(2): 241–260, 2024, doi: 10.24423/cames.2024.448

This article belongs to the *Special Issue on Scientific Computing and Learning Analytics for Smart Healthcare Systems* edited by Dr. C. Chakraborty, Dr. S. Barbosa and Dr. L. Garg

Classification of Cognitive States Using Clustering-Split Time Series Framework

J. Siva RAMAKRISHNA[1)*], Hariharan RAMASANGU[2)]

[1)] *Institute of Aeronautical Engineering, Hyderabad, India*

[2)] *Relecura Inc., Bangalore, India; e-mail: rharihar@ieee.org*

[*] *Corresponding Author e-mail: jsrkrishna3@gmail.com*

Over the last two decades, functional Magnetic Resonance Imaging (fMRI) has provided immense data about the dynamics of the brain. Ongoing developments in machine learning suggest improvements in the performance of fMRI data analysis. Clustering is one of the critical techniques in machine learning. Unsupervised clustering techniques are utilized to partition the data objects into different groups. Supervised classification techniques applied to fMRI data facilitate the decoding of cognitive states while a subject is engaged in a cognitive task. Due to the high dimensional, sparse, and noisy nature of fMRI data, designing a classifier model for estimating cognitive states becomes challenging. Feature selection and feature extraction techniques are critical aspects of fMRI data analysis. In this work, we present one such synergy, a combination of Hierarchical Consensus Clustering (HCC) and the Statistics of Split Timeseries (SST) framework to estimate cognitive states. The proposed HCC-SST model's performance has been verified on StarPlus fMRI data. The obtained experimental results show that the proposed classifier model achieves 99% classification accuracy with a smaller number of voxels and lower computational cost.

Keywords: functional MRI data, classification, consensus clustering, SVM classifier, GNB classifier, XGBoost.

1. Introduction

Machine learning classifier models, such as unsupervised and supervised techniques, have been used to analyze fMRI over the past couple of decades. In human brain diagnosis, there are numerous imaging modalities. These brain imaging modalities are functional and structural imaging modalities, and among them functional MRI provides functional information about the brain. Functional brain imaging modalities are useful in diagnosing human brain-related disorders such as epilepsy, brain tumors, Alzheimer's disease, and Parkinson's

disease. The brain image sequence in fMRI data consists of Hemodynamic Response Function (HRF), expressed in terms of Blood Oxygen Level Dependent (BOLD) signal at different time intervals [1].

The fMRI method is a noninvasive brain imaging technique for diagnosing the human brain. The brain imaging modality detects neural responses with the help of the BOLD signal contrast [2]. Additionally, fMRI plays a crucial role in neuroscience research for analyzing human brain activity associated with cognition or perception. The dimensionality of fMRI is a significant issue in fMRI image classification. Machine intelligence algorithms are developed for cognitive state classification and functional connectivity analysis using fMRI data [3]. In general, fMRI data consists of several brain Regions of Interest (ROIs). Each region of the brain comprises a few thousand voxels. Because of the large fMRI data dimensionality, classification or decoding the human brain states becomes more challenging. In the context of healthcare data analysis, the development of computational algorithms is essential [4, 5]. Therefore, the selection of relevant voxels is a critical challenge in fMRI data analysis.

Cognitive activities in the human brain have been analyzed using different machine intelligence algorithms, such as clustering and classification techniques [6]. Clustering is an unsupervised machine learning algorithm, and classification of objects is a supervised learning technique. The image sequences in the fMRI data consist of a voxel time course. The fMRI data for a particular human subject comprises a set of ROIs. A critical challenge in classifying cognitive states using fMRI data is determining the ROIs that are responsive to a particular cognitive task. In general, clustering algorithms segment the brain regions using fMRI data. In general, hybrid clustering algorithms provide stable clustering groups in fMRI data with the help of multiple base clustering techniques [7, 8]. Partitioning the brain regions using fMRI data is an unsupervised data analysis problem. The machine learning classifier performance depends on the attributes used to build the classifier [9]. The selection of appropriate features is essential for efficient analysis of fMRI data. The standard approach used for evaluating the choice of a subset of features is classification accuracy. The selection of relevant features holds many implications for the fMRI data analysis problem.

In general, fMRI data features a limited number of samples but a higher number of significant observations. Thus, there is a need for appropriate feature selection and feature extraction techniques that will help in selecting stable features across fMRI data. Clustering and classification problems are generally viewed as independent components in data analysis. In this work, we consider a two-phase approach for cognitive state classification. The first phase involves the application of clustering techniques to fMRI data to partition the fMRI data into multiple groups and select relevant features (voxels). In the second phase,

statistical features are extracted to develop a machine-learning classifier for cognitive state classification. In this work, we employ HCC in conjunction with statistics of a split time series framework to decode human brain states. The proposed classification framework improves classification accuracy with a minimum number of voxels as features. The rest of the article includes a background provided in Sec. 2. Section 3 discusses related work. Section 4 presents the proposed clustering-split time series framework. The obtained classification results are elaborated in Sec. 5, and finally, conclusion is provided in Sec. 6.

2. Background

The two fundamental approaches for fMRI data analysis include: 1) mapping the brain states while subjects perform a particular cognitive task, and 2) segmenting brain regions into various clusters [10]. Classification of data samples is considered a supervised learning technique. The fMRI dataset consists of voxel instances. The instances in the dataset used by the classifier are denoted as features. These features are generally independent and individual variables within the dataset. Classifiers are a tangible implementation of pattern recognition in the form of the classification of objects. Classification algorithms map unlabeled data samples to a particular category or class.

On the other hand, unsupervised clustering algorithms identify similar groups in the dataset [11]. Clustering algorithms partition the data objects into different groups based on distance metrics or a similarity measure between the data objects. The objects present in the group are similar to the objects in the same group but different from those in the other group. Clustering algorithms are broadly categorized into three types: 1) unsupervised clustering, 2) supervised clustering, and 3) semi-supervised clustering.

In general, basic clustering algorithms are unsupervised. The clustering algorithms consider a set of unlabeled objects and group them into a specific number of clusters without considering any labels of the objects. In clustering algorithms, the cluster centroid identifies these clusters. Unsupervised clustering techniques lack knowledge of the relationship between objects present in the dataset and rely on distance metrics or similarity measures for clustering.

Similarity measures play a crucial role in computing the similarity between the data objects. The distance measure used in clustering algorithms quantifies the similarity between two objects. It represents similarity or dissimilarity between the objects [12]. A smaller distance between the objects indicates high similarity, while a greater distance between the objects suggests low similarity. Therefore, the main requirement of similarity metric calculation is to obtain an appropriate similarity or distance function [13].

2.1. Similarity measures

There are various types of standard distance metrics, which are discussed below. The similarity measures are usually probability distribution-based and metric-based techniques.

2.1.1. Euclidean distance. The metric used for comparing two data vectors y_{1i} and y_{2i} is given by Eq. (1). The index i iterates over all values in the data vector. The distance metric provides the geometric distance between two objects:

$$d_e = \sqrt{\sum_{i=1}^{n} (y_{1i} - y_{2i})^2}. \tag{1}$$

2.1.2. Manhattan distance. It is similar to Euclidian distance and calculated by considering the sum of the absolute distance between the two data vectors, as represented in Eq. (2):

$$d_M = \sum_{i=1}^{n} (y_{1i} - y_{2i}). \tag{2}$$

2.1.3. Pearson's correlation. The expression for Pearson's correlation coefficient r is expressed as shown in Eq. (3):

$$r = \frac{\sum_{i=1}^{n} (y_{1i} - \overline{y}_1)(y_{2i} - \overline{y}_2)}{\sqrt{\sum_{i=1}^{n} (y_{1i} - \overline{y}_1)} \sqrt{\sum_{i=1}^{n} (y_{2i} - \overline{y}_2)}}, \tag{3}$$

where $\overline{y}_1$ is the mean vector of y_1 and $\overline{y}_2$ is the mean vector of y_2. The metric measures provide the tendency of vectors to increase or decrease together. The metric ranges from -1 to 1. A value -1 indicates that the vectors are negatively correlated and opposite, 0 represents no correlation and independent vectors, and 1 indicates that the vectors are positively correlated and identical to each other. Clustering algorithms use these similarity metrics as distance metrics for partitioning data into multiple groups. Popular and commonly used clustering techniques include hierarchical clustering, k-means clustering, and spectral clustering. In this work, we consider the HCC algorithm for partitioning fMRI data into different groups.

2.1.4. Hierarchical consensus clustering. HCC is also known as clustering aggregation or cluster ensemble. The algorithm aims to determine a single partitioning of data from several existing base clusterings [14]. It has been accepted that CC can assist in finding unusual clusters, generate robust clustering results, handle outliers, sample variations, and noise, and combine solutions from various attributes or features. HCC is considered a combinatorial optimization problem, and it is proven to be NP-complete. Several algorithms have been proposed to address computational challenges, including graphbased techniques, co-association matrix-based clustering techniques, and prototype-based techniques.

HCC employs base clustering techniques to obtain various groupings for a given set of observations using various initializations. Then, the consensus clustering (CC) identifies robust clusters across these partitions. The obtained partitions are insensitive to the initialization of the fundamental clustering algorithms. These clustering groups are determined through:

1) Applying different base clustering techniques.
2) Applying a similar clustering algorithm with different parameters.
3) Using clustering algorithm with various distance metrics.
4) Employing various clustering initializations of a similar clustering algorithm.
5) Using various attributes of the data.
6) Combining some or all of the above.

The HCC generates different data partitions using base clustering techniques, such as k-means, hierarchical, and spectral clustering, each with various initializations for different clusters. The segmentation of human brain regions using fMRI data is treated as a clustering problem. The clustering algorithms discussed above group voxels into different clusters with low inter-cluster and high intra-cluster similarity [15].

Clustering algorithms are used to segment human brain regions (ROIs) with the help of fMRI data. The selection of features (voxels) from the fMRI dataset is an important activity in classifying brain states. In general, voxels in the dataset have a time series, which is considered as a feature. Given that the fMRI dataset is generally high-dimensional, much research is directed toward dimensional reduction and voxel selection (feature selection) [16]. In this work, we use HCC to select voxels as features for classifying cognitive states. First, voxels are selected randomly from each group. Then, the obtained voxels are split into two halves and the statistical average or mean is computed for each half.

In general, feature extraction techniques [17] are employed to generate new attributes to build a classifier for cognitive state classification. Usually, the size or dimension of fMRI data, including both spatial and temporal dimensions, is high, often in terms of a few thousand. Statistics is the field of science that

focuses on collecting, analyzing, and drawing conclusions from data. Statistical techniques are used to summarize, organize, and draw conclusions from data. Therefore, familiarity with statistical literacy and statistical methods is vital in data analysis. Fundamental statistical parameters, such as the mean, are computed for each half of the voxel time series.

2.1.5. Mean or average. One category of statistical parameters determines how a set of numbers is centered around a specific point. This category of parameters is called central tendency. The most familiar parameter of this type is the average or mean. The parameter mean is represented as the arithmetic average of a set of numbers. The mean provides an indication of where the center lies for a given set of numbers. The statistical mean is determined by considering the objects or numbers in the given set. The formula for the statistical mean is given in Eq. (4):

$$\overline{y} = \frac{\sum_{i=1}^{n} y_i}{N}, \tag{4}$$

where $\overline{y}$ is the mean – the cumulative sum of all the numbers in the dataset and N is the total number of observations present in the data. The statistical mean is the most standard measure of central tendency.

2.1.6. Standard deviation. Standard deviation provides an approximate average quantity. Every number in a dataset varies from the center. Statisticians consider the standard deviation as a good measure of variation, especially in inferential statistics. There are two different expressions for standard deviation, one for the sample standard deviation, which is given in Eq. (5):

$$S = \sqrt{\frac{\sum (y_i - \overline{y})^2}{N-1}}, \tag{5}$$

where S represents the standard deviation, and the other for the population standard deviation, as given in Eq. (6):

$$\sigma = \sqrt{\frac{\sum (y_i - \overline{y})^2}{N}}. \tag{6}$$

In the sample standard deviation, $N-1$ is in the denominator, and the correction of -1 is added to correct bias. The correction makes the value of sample standard deviation more significant than the population standard deviation. In general, statisticians work with sample standard deviation rather than population standard deviation.

2.1.7. Variance. Variance is a measure of variation, and it has some mathematical relationship with standard deviation. It is represented as the average of the square of the standard deviation. In other words, variance has the same formula as we use for standard deviation except the absence of the square root in the final expression. The expression for sample variance is given in Eq. (7):

$$S^2 = \frac{\sum (y_i - \overline{y})^2}{N-1}. \tag{7}$$

The expression for population variation is given in Eq. (8):

$$\sigma^2 = \frac{\sum (y_i - \overline{y})^2}{N}, \tag{8}$$

where S^2 is the sample variance, and σ^2 is the population variance. Variance is a quite frequently used parameter in inferential statics. However, due to its conceptual drawbacks (square in the formula), standard deviation is more prevalent in inferential and descriptive statistics.

3. Related work

In this section, we discuss the related machine intelligence models for different feature selection and classification algorithms for decoding human brain states. In the literature, researchers have proposed techniques for analyzing fMRI data [10, 18, 19]. Computational approaches of Genetic Algorithm (GA) and Particle Swarm Optimization (PSO) are widely used techniques for fMRI data analysis [20, 21]. For instance, a GA based on entropy and a linear collaborative discriminant regression hybrid framework is applied to find the maximum significant voxels [22]. The stable feature selection is an important criterion for model selection in classifying cognitive states [23]. The whole-brain fMRI data is partitioned into three-dimensional volumes called voxels. The most appropriate voxels as features are obtained from symmetrical uncertainty based on the entropy framework for decoding the brain states [24]. In all these studies, machine intelligence techniques are used to decode human brain states using fMRI data.

A constrained spatiotemporal independent component analysis technique, based on multi-objective optimization, is applied to real and simulated fMRI data [25]. This method is able to perform source recovery from fMRI data. However, deep learning techniques that decode the cognitive states from fMRI data are hindered by high dimensionality and a small sample size. In this context, the transfer learning framework provides a solution to some extent [26]. The functional connectivity concept is considered as an important tool for the classification of fMRI data. A parcellation technique provides a measure of node-to-functional network assignment changes across cognitive states and subjects.

Using fMRI data obtained across several cognitive tasks is considered to demonstrate the connectivity changes. The technique achieves an average accuracy of 97% [27]. The fMRI brain imaging modality is able to determine the activation of brain regions and functional connectivity among them. The interest in the use of functional brain imaging modalities along with machine intelligence is gaining increasing interest. Machine learning techniques hold significant potential for understanding and diagnosing brain-related disease progress [28]. A dynamic graph learning technique was employed for generating an ensemble of dynamic graph that helps in developing brain networks for the classification of cognitive states [29]. The multidomain brain decoder learns the spatiotemporal changes in brain response within a specific time window. A model performance was evaluated using task-based fMRI data with an accuracy of 90% [30].

The voxel selection process is categorized into the wrapper method and the filter method. The filter method achieves the selection of relevant voxels using relevance measures. In the case of the wrapper method, the optimized feature subsets are obtained for feature selection. The attributes present in fMRI data in connection with a particular ROI are typically obtained. In this work, we consider HCC in conjunction with SST series for decoding human brain states. The proposed classification framework improves the classification accuracy values using a minimum number of voxels as features. Further details of the proposed framework are elaborated on in the next section.

4. Proposed clustering-split time series framework

Machine intelligence techniques, such as clustering and classification, are applied separately for the fMRI data analysis. In this study, we develop a novel classification framework for the estimation of human brain states. The framework considers a hierarchical clustering algorithm for voxel selection, followed by statistical features extracted from the selected voxels. Machine learning classifiers are then developed using these extracted features for decoding human brain states. This approach produces few voxels as attributes for decoding human brain states. The functional block diagram of the proposed clustering split time series framework is given in Fig. 1. The clusteringsplit time series model applies various base clustering techniques to voxel time series. Voxels are randomly selected from clusters, split into two halves, and then statistical features are extracted from each half. Feature vectors are next formed from the obtained statistical features. Finally, the obtained feature vectors are applied as input to the Gaussian naive Bayes (GNB), XGBoost, and Support Vector Machine (SVM) classifiers. The classification accuracy of the three classifiers is compared for cognitive state classification. A detailed description of the steps involved in the framework is given below.

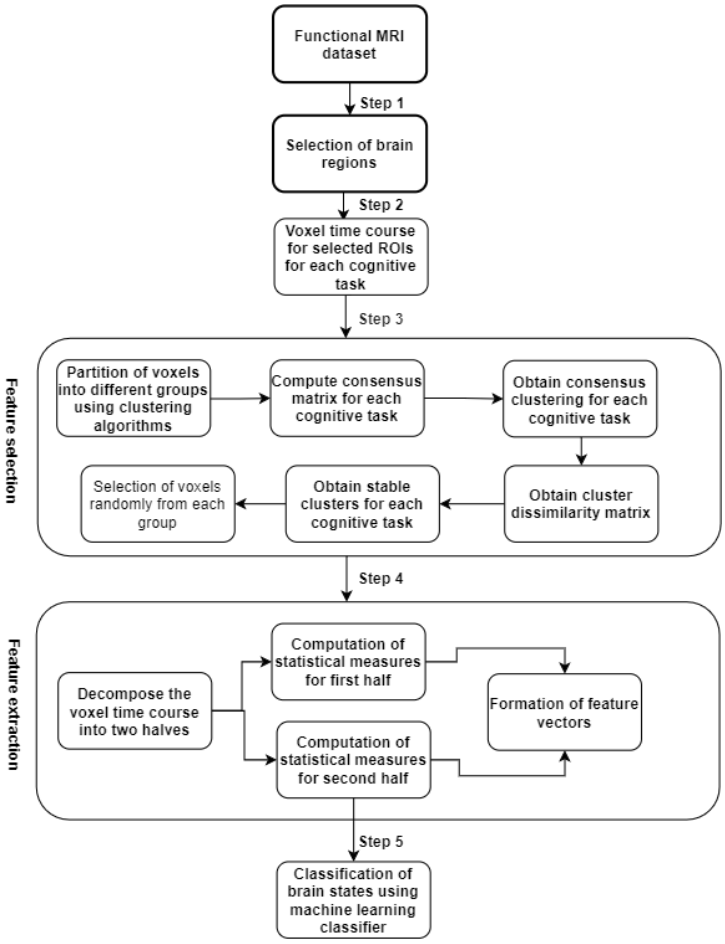

FIG. 1. Proposed HCC-SST framework for cognitive state classification framework.

Step 1: Select the brain regions.

In general, fMRI data consists of several ROIs with a specific number of trials. Each ROI comprises a certain number of voxels. Therefore, it is always difficult to run the algorithm with whole-brain data. Hence, the framework begins with the selection of a specific number of ROIs.

Step 2: Extract the voxel time course for selected ROIs for each cognitive task.

The time series of voxels is extracted for the selected ROIs across various cognitive tasks. For example, let $T1$ and $T2$ be voxel time courses for two cognitive tasks within a specific fMRI image sequence. One of the critical features of the proposed clustering-split time framework is the clustering performed based on a single trial data or image sequence to select voxels for the remaining trial data.

Step 3: Select the voxels as features from different clusterings or groups.

HCC is applied to voxel time series data for each cognitive task. HCC provides robust clusters for a given fMRI data by employing fundamental clustering algorithms to partition the functional MRI data. The fundamental clustering technique is chosen as k-means, hierarchical, and spectral clustering algorithms. The base clustering techniques are applied for a specific number of clusters $k = 2$ to 10, which means that for every k, ten numbers of fundamental clusterings with various initializations are obtained. The consensus matrix C_{Dk} is defined for each clustering and dataset, where D denotes a pair of cognitive data represented as *dataP* and *dataS*. C_{Dk} is also known as the average consensus matrix. The similarity between different partitions is obtained using the average consensus matrix C_{Dk}. The (i, l)-th entry of C_{Dk} is given in Eq. (9):

$$C_{Dk} = \frac{n_{il}}{N}, \tag{9}$$

where n_{il} denotes the number of times voxels are clustered together in a similar group, and N represents the number of clustering partitions. If the value of C_{Dk} is equal to or close to one, voxels are clustered together in a similar group. If the value of C_{Dk} is far from one or close to zero, voxels are not clustered together in a similar group. Hierarchical average link-based CC is applied over C_{Dk} for each k and each cognitive dataset. For each cluster, dissimilarity is obtained with the help of various dissimilarity measures. These measures include: 1) variation of information (VI), 2) normalized variation of information (NVI), 3) normalized mutual information (NMI), and 4) rand index (RI). These dissimilarity measures are used to determine the optimal dissimilarity among the pair of cognitive datasets, and k^* is determined as the optimal number of stable clusters.

The normalized mutual information finds the dissimilarity between two partitions, as given in Eq. (10):

$$\mathrm{NMI}(L_{i,k},\, L_{j,k}) = \frac{2\mathrm{I}(L_{i,k},\, L_{j,k})}{\mathrm{H}(L_{i,k}) + \mathrm{H}(L_{j,k})}, \tag{10}$$

where $L_{i,k}$ and $L_{j,k}$ represent the voxel labels for the pair of cognitive tasks $\mathrm{I}(L_{i,k},\, L_{j,k})$ represents the mutual information, and $\mathrm{H}(L_{i,k})$ and $\mathrm{H}(L_{j,k})$ represent the entropy of the voxels. The two partitions are considered to be similar if the value of NMI is one, and they dissimilar if the value of NMI is zero.

The dissimilarity measure variation of information between two partitions is given in Eq. (11):

$$\mathrm{VI}(L_{i,k},\, L_{j,k}) = \mathrm{H}(L_{i,k}) + \mathrm{H}(L_{j,k}) - 2\mathrm{I}(L_{i,k},\, L_{j,k}). \tag{11}$$

The maximum value of VI is considered a measure to select the optimal number of clusters.

The normalized variation of information between the two partitions is given in Eq. (12):

$$\mathrm{NVI}(L_{i,k},\, L_{j,k}) = \frac{\mathrm{VI}}{\mathrm{M}}, \tag{12}$$

where M represents the number of voxels in the partition, and the maximum value of the metric is considered for selecting the optimal number of clusters.

The RI metric compares dissimilarity among pairs of partitions as follows:

$$\mathrm{RI}(L_{i,k},\, L_{j,k}) = \frac{n_{11} + n_{00}}{n_{00} + n_{10} + n_{01} + n_{11}}. \tag{13}$$

In Eq. (13), n_{11} denotes the number of pairs of voxels present in a similar partition, n_{10} and n_{01} denote the number of voxels in the similar cluster in one partition and different in the other partition, and n_{00} represents the number of voxels in different clusters. The minimum value of RI is used as a metric for determining the optimal cluster. The optimal number of clusters (k^*) is obtained by comparing dissimilarity among the partitions. Voxels are randomly selected from each group for a given pair of cognitive datasets. The selected few voxels are applied as input to the statistics split time series framework.

Step 4: Extract statistical features for selected voxels.

The statistical measure mean or average is calculated for each voxel. According to the principle of fMRI, the voxel time course is delayed in nature. The voxel time series is partitioned into two halves. The mean value of each voxel time series is determined as follows:

$$m_1 = \frac{2}{L} \sum_{i=1}^{L/2} V(i), \tag{14}$$

$$m_2 = \frac{2}{L} \sum_{i=\frac{L}{2}+1}^{L} V(i), \tag{15}$$

where m_1 represents the mean value for the first half of the voxel time series. Similarly, m_2 represents the mean value for the second half of the voxel time course. Finally, the mean vector M for a given voxel is determined by appending m_1 and m_2, i.e., $\mathrm{M} = [m_1 m_2]$. From the obtained values of M feature vectors are then generated.

Step 5: Machine learning classifiers are built for the classification of cognitive states or decoding brain states.

The feature vectors generated in Step 4 are used to develop machine learning classifiers such as the GNB classifier, SVM classifier, and XGBoost classifier.

5. Results and discussion

The performance of the proposed HCC-SST framework is evaluated using the standard StarPlus fMRI dataset. This section elaborates on experimental results obtained for the proposed classification model. The proposed framework performance is examined on six healthy subjects from the StarPlus fMRI dataset. The dataset consists of six subjects. Each subject is identified by a unique ID number: subject 05680, subject 04847, subject 04820, subject 05675, subject 05710, and subject 04799 [31]. Three machine learning classifiers are built and compared to verify the performance of the proposed model. The classifiers are: SVM, GNB, and XGBoost and are applied to the classification of cognitive states. Leave-one-out-cross validation (LOOCV) is performed using the obtained features.

Secondly, the classifiers are built in five ways: 1) using whole-brain data (all ROIs), 2) using the seven most important brain regions (LIPS, LDLPFC, CALC, LIPL, LT, LTRIA, and LOPER) as highlighted in the dataset, 3) using seven significant ROIs with HCC, 4) using seven significant ROIs with SST, and 5) using seven significant ROIs with proposed HCC-SST framework. Finally, the classification accuracy of classifiers is compared.

The proposed framework is a two-phase approach for cognitive state classification. HCC is applied to each subject in the first level and selects a few voxels. Then, in the next level, statistical mean features are extracted. The voxels chosen in the first level have a definite standard time course, represented by several time instants.

The length of the voxel time course is split into two halves, and mean values are calculated for each half of the time series. The obtained statistical mean values are used as attributes to build a machine-learning classifier. The results obtained for six subjects in the StarPlus fMRI dataset are shown in Tables 1, 2, 3, 4, 5, and 6. Also, the classification accuracy results for each classifier are compared.

Three classifiers are built using voxels from the entire brain (considering voxels from all 25 ROIs) and the seven most important brain regions, as highlighted in the StarPlus dataset. The obtained classification accuracy results of the proposed framework are compared with the HCC feature selection framework [32] and SST series feature extraction framework [33].

Table 1 presents the obtained classification accuracy results for subject 04799. A total of 4949 voxels are available for subject 04799. The classifiers are built using LOOCV with all the available voxels as features. The results obtained are 87%, 90%, and 97% for the GNB classifier, SVM classifier, and XGBoost classifier, respectively. Subject 04799 consists of 1884 voxels for the seven most significant brain regions. The classifiers are built for these selected voxels. The classifiers are trained and tested with 1884 voxels. The classification results

Table 1. Classifier performance for subject 04799.

S. No.	Machine learning classifier	Criteria	Voxels	Accuracy [%]
1	GNB (all ROIs)	without CC and SST	4949	87
2	GNB (seven ROIs)	without CC and SST	1884	86
3	GNB (all ROIs)	with CC	530	85
4	GNB (seven ROIs)	with SST	1884	88
5	GNB (seven ROIs)	with CC and SST	80	85
6	SVM (all ROIs)	without CC and SST	4949	90
7	SVM (seven ROIs)	without CC and SST	1884	92
8	SVM (seven ROIs)	with CC	530	80
9	SVM (seven ROIs)	with SST	1884	98
10	SVM (seven ROIs)	with CC and SST	80	95
11	XGBoost (all ROIs)	without CC and SST	4949	97
12	XGBoost (all ROIs)	without CC and SST	1884	96
13	XGBoost (all ROIs)	with CC	530	84
14	XGBoost(all ROIs)	with SST	1884	84
15	XGBoost (all ROIs)	with CC and SST	80	88

obtained are 86%, 92%, and 96% for GNB, SVM, and XGBoost, respectively. A total of 530 voxels are selected from CC for the seven most important brain regions. The classifiers are trained and tested with the help of 530 voxels. The classification accuracy results obtained are 85%, 80%, and 84% for GNB, SVM, and XGBoost classifiers, respectively. Next, SST series concept is executed on the seven best ROIs. The obtained classification accuracy results are 88%, 98%, and 84% for the GNB classifier, SVM classifier, and XGBoost classifier. The proposed HCC-SST series is verified to the seven most important ROIs of subject 04799. A total of 80 voxels are selected from HCC. In the second phase, statistical mean values are computed for each voxel as features. Machine learning classifiers are built with these features. The obtained classification accuracy results are 85%, 95%, and 88% for the GNB classifier, SVM classifier, and XGBoost classifier, respectively.

Table 2 presents the obtained classification accuracy results for subject 04847. A total of 4098 voxels is available for subject 04848. The classifiers are trained and LOOCV is performed with the help of all existing voxels as features. The obtained results are 94%, 99%, and 97% for GNB, SVM, and XGBoost classifiers, respectively. Subject 04847 consists of 1714 voxels for the seven most significant brain regions. Machine learning classifiers are built for these selected voxels. The classifiers are trained and tested with 1714 voxels. The classification accuracy results obtained are 95%, 99%, and 95% for GNB, SVM, and XGboost, respec-

Table 2. Classifier performance for subject 04847.

S. No.	Machine learning classifier	Criteria	Voxels	Accuracy [%]
1	GNB (all ROIs)	without CC and SST	4098	94
2	GNB (seven ROIs)	without CC and SST	1714	95
3	GNB (all ROIs)	with CC	174	92
4	GNB (seven ROIs)	with SST	1714	90
5	GNB (seven ROIs)	with CC and SST	80	99
6	SVM (all ROIs)	without CC and SST	4098	99
7	SVM (seven ROIs)	without CC and SST	1714	99
8	SVM (seven ROIs)	with CC	174	90
9	SVM (seven ROIs)	with SST	1714	98
10	SVM (seven ROIs)	with CC and SST	80	99
11	XGBoost (all ROIs)	without CC and SST	4098	97
12	XGBoost (all ROIs)	without CC and SST	1714	95
13	XGBoost (all ROIs)	with CC	174	92
14	XGBoost(all ROIs)	with SST	1714	90
15	XGBoost (all ROIs)	with CC and SST	80	92

tively. A total of 174 voxels are selected from CC for the seven most important brain regions. The classifiers are built and tested with 174 voxels. The classification accuracy results obtained are 92%, 90%, and 92% for the GNB classifier, SVM classifier, and XGBoost classifier, respectively. Next, SST series concept is executed on the seven best ROIs. The obtained classification accuracy results are 90%, 98%, and 90% for the GNB, SVM, and XGBoost classifiers, respectively. The proposed HCC-SST series is verified on the seven most important ROIs of subject 04847. A total of 80 voxels are selected from HCC. In the second phase, statistical mean values are computed for each voxel as features. Machine learning classifiers are built with these features. The obtained classification accuracy results are 99%, 99%, and 92% for GNB, SVM, and XGBoost classifiers, respectively.

Similarly, Tables 3, 4, 5, and 6 elaborate on the obtained classification accuracy results for subjects 04820, 05710, 05680, and 05675, respectively. Among the experiments conducted, the proposed classification framework achieves 98%, 99%, and 90% accuracy with 140 voxels for subject 04820 (Table 3). The proposed model achieves 95%, 99%, and 98% with 100 voxels for subject 05710 (Table 4). The proposed model achieves 90%, 99%, 99% with 220 voxels for the subject 05680 (Table 5).

The classification accuracy of 95%, 99%, and 90% is obtained with 80 voxels using the GNB, SVM, and XGBoost classifiers, respectively. Table 7 compares

Table 3. Classifier performance for subject 04820.

S. No.	Machine learning classifier	Criteria	Voxels	Accuracy (%)
1	GNB (all ROIs)	without CC and SST	5015	94
2	GNB (seven ROIs)	without CC and SST	1741	92
3	GNB (all ROIs)	with CC	595	80
4	GNB (seven ROIs)	with SST	1741	90
5	GNB (seven ROIs)	with CC and SST	140	98
6	SVM (all ROIs)	without CC and SST	5015	99
7	SVM (seven ROIs)	without CC and SST	1741	98
8	SVM (seven ROIs)	with CC	595	76
9	SVM (seven ROIs)	with SST	1741	82
10	SVM (seven ROIs)	with CC and SST	140	99
11	XGBoost (all ROIs)	without CC and SST	5015	94
12	XGBoost (all ROIs)	without CC and SST	1741	88
13	XGBoost (all ROIs)	with CC	595	84
14	XGBoost(all ROIs)	with SST	1741	88
15	XGBoost (all ROIs)	with CC and SST	140	90

Table 4. Classifier performance for subject 05710.

S. No.	Machine learning classifier	Criteria	Voxels	Accuracy [%]
1	GNB (all ROIs)	without CC and SST	4634	95
2	GNB (seven ROIs)	without CC and SST	1884	88
3	GNB (all ROIs)	with CC	610	92
4	GNB (seven ROIs)	with SST	1884	90
5	GNB (seven ROIs)	with CC and SST	100	95
6	SVM (all ROIs)	without CC and SST	4634	99
7	SVM (seven ROIs)	without CC and SST	1884	99
8	SVM (seven ROIs)	with CC	610	90
9	SVM (seven ROIs)	with SST	1884	95
10	SVM (seven ROIs)	with CC and SST	100	99
11	XGBoost (all ROIs)	without CC and SST	4634	95
12	XGBoost (all ROIs)	without CC and SST	1884	95
13	XGBoost (all ROIs)	with CC	610	94
14	XGBoost(all ROIs)	with SST	1884	94
15	XGBoost (all ROIs)	with CC and SST	100	98

Table 5. Classifier performance for subject 05680.

S. No.	Machine learning classifier	Criteria	Voxels	Accuracy [%]
1	GNB (all ROIs)	without CC and SST	5062	99
2	GNB (seven ROIs)	without CC and SST	2031	97
3	GNB (all ROIs)	with CC	520	90
4	GNB (seven ROIs)	with SST	2031	96
5	GNB (seven ROIs)	with CC and SST	220	90
6	SVM (all ROIs)	without CC and SST	5062	99
7	SVM (seven ROIs)	without CC and SST	2031	99
8	SVM (seven ROIs)	with CC	520	89
9	SVM (seven ROIs)	with SST	2031	96
10	SVM (seven ROIs)	with CC and SST	220	99
11	XGBoost (all ROIs)	without CC and SST	5062	96
12	XGBoost (all ROIs)	without CC and SST	2031	98
13	XGBoost (all ROIs)	with CC	520	90
14	XGBoost(all ROIs)	with SST	2031	94
15	XGBoost (all ROIs)	with CC and SST	220	99

Table 6. Classifier performance for subject 05675.

S. No.	Machine learning classifier	Criteria	Voxels	Accuracy [%]
1	GNB (all ROIs)	without CC and SST	5134	88
2	GNB (seven ROIs)	without CC and SST	2061	90
3	GNB (all ROIs)	with CC	580	92
4	GNB (seven ROIs)	with SST	2061	88
5	GNB (seven ROIs)	with CC and SST	80	95
6	SVM (all ROIs)	without CC and SST	5134	99
7	SVM (seven ROIs)	without CC and SST	2061	99
8	SVM (seven ROIs)	with CC	580	90
9	SVM (seven ROIs)	with SST	2061	97
10	SVM (seven ROIs)	with CC and SST	80	99
11	XGBoost (all ROIs)	without CC and SST	5134	92
12	XGBoost (all ROIs)	without CC and SST	2061	88
13	XGBoost (all ROIs)	with CC	580	90
14	XGBoost(all ROIs)	with SST	2061	86
15	XGBoost (all ROIs)	with CC and SST	80	90

Table 7. Comparison of classifier performance.

S. No.	Subject	Parameter	Gupta and Chatur [22]	Ranjan *et al.* [24]	Proposed HCC-SST technique
1	04799	No. of voxels	482	61	80
		Accuracy	97	90	**99**
2	04847	No. of voxels	2045	39	80
		Accuracy	95	95	**99**
3	04820	No. of voxels	2354	46	140
		Accuracy	98	95	**98**
4	05710	No. of voxels	2075	44	100
		Accuracy	96	93	**99**
5	05680	No. of voxels	2474	40	220
		Accuracy	97	90	**99**
6	05675	No. of voxels	2140	60	80
		Accuracy	97	97	**99**

the proposed method with existing techniques applied to a similar dataset. The results are compared with Gupta and Chatur [22] and Ranjan *et al.* [24]. It is observed that the proposed HCC-SST time series framework performs both feature selection and feature extraction for cognitive state classification. Furthermore, the proposed framework achieves good classification accuracy with a minimum number of voxels and smaller computational cost, without deep learning architecture, when compared to existing techniques.

6. Conclusions

An efficient classification framework based on HCC and SST was proposed in this paper. The proposed classification algorithm selected the stable features from fMRI dataset. The proposed algorithm aimed to choose the minimum number of voxels to reduce computational time while decoding the brain states. The time course of selected voxels was split into two halves, and the statistical mean was computed for each half of the voxel time course. The extracted features are used to build a classifier for cognitive state classification. The performance of the proposed framework was examined on six subjects in the StarPlus fMRI database. For six subjects in the StarPlus fMRI dataset, the obtained classifier results are compared with existing cognitive state classification results. The results demonstrate that the proposed HCC-SST technique outperforms the results reported in the existing techniques by achieving higher accuracy. The experimental

results show that the proposed approach has scored 99% accuracy with a reduced number of voxels and lower computational cost compared to existing methods.

References

1. O.J. Arthurs, S. Boniface, How well do we understand the neural origins of the fMRI BOLD signal, *Trends in Neurosciences*, **25**(1): 27–31, 2002, doi: 10.1016/S0166-2236(00)01995-0.
2. N.K. Logothetis, B.A. Wandell, Interpreting the BOLD signal,*Annual Reviews in Physiology*, **66**: 735–769, 2004, doi: 10.1146/annurev.physiol.66.082602.092845.
3. T.M. Mitchell, R. Hutchinson, M.A. Just, R.S. Niculescu, F. Pereira, X. Wang, Classifying instantaneous cognitive states from fMRI data, [in:] *American Medical Informatics Association Annual Symposium Proceedings*, pp. 465–469, 2003, PMID: PMC1479944, https://pubmed.ncbi.nlm.nih.gov/14728216.
4. A. Kishor, C. Chakraborty, W. Jeberson, Reinforcement learning for medical information processing over heterogeneous networks, *Multimedia Tools and Applications*, **80**: 23983–24004, 2021, doi: 10.1007/s11042-021-10840-0.
5. A. Kishor, C. Chakarbarty, Task offloading in fog computing for using smart ant colony optimization, *Wireless Personal Communications*, **127**: 1683–1704, 2021, doi: 10.1007/s11277-021-08714-7.
6. F. De Martino, G. Valente, N. Staeren, J. Ashburner, R. Goebel, E. Formisano, Combining multivariate voxel selection and support vector machines for mapping and classification of fMRI spatial patterns, *Neuroimage*, **43**(1): 44–58, 2008, doi: 10.1016/j.neuroimage.2008.06.037.
7. A.L. Fred, A.K. Jain, Combining multiple clusterings using evidence accumulation, *IEEE Transactions on Pattern Analysis and Machine Intelligence*, **27**(6): 835–850, 2005, doi: 10.1109/TPAMI.2005.113.
8. S. Ryali, T. Chen, A. Padmanabhan, W. Cai, V. Menon, Development and validation of consensus clustering-based framework for brain segmentation using resting fMRI, *Journal of Neuroscience Methods*, **240**: 128–140, 2015, doi: 10.1016/j.jneumeth.2014.11.014.
9. J. Tang, S. Alelyani, H. Liu, Feature selection for classification: A review, [in:] *Data Classification: Algorithms and Applications*, C.C. Aggarwal [Ed.], CRC Press, New York, pp. 37–64, 2014.
10. J.D. Cohen *et al.*, Computational approaches to fMRI analysis, *Nature Neuroscience*, **20**(3): 304–313, 2017, doi: 10.1038/nn.4499.
11. D.R. Hardoon, J. Mourão-Miranda, M. Brammer, J. Shawe-Taylor, Unsupervised analysis of fMRI data using kernel canonical correlation, *NeuroImage*, **37**(4): 1250–1259, 2007, doi: 10.1016/j.neuroimage.2007.06.017.
12. R. Xu, D. Wunsch, Survey of clustering algorithms, *IEEE Transactions on Neural Networks*, **16**(3): 645–678, 2005, doi: 10.1109/TNN.2005.845141.
13. R. Agrawal, C. Faloutsos, A. Swami, Efficient similarity search in sequence databases, [in:] *Lecture Notes in Computer Science*, Vol. 730, pp. 69–84, 1993, doi: 10.1007/3-540-57301-1_5.

14. S. Monti, P. Tamayo, J. Mesirov, T. Golub, Consensus clustering: a resampling-based method for class discovery and visualization of gene expression microarray data, *Machine Learning*, **52**(1): 91–118, 2003, doi: 10.1023/A:1023949509487.

15. K. Kim, R.I. McKay, B.R. Moon, Multi objective evolutionary algorithms for dynamic social network clustering, [in:] *GECCO '10: Proceedings of the 12th Annual Conference on Genetic and Evolutionary Computation*, pp. 1179–1186, 2010, doi: 10.1145/1830483.1830699.

16. V. Michel, C. Damon, B. Thirion, Mutual information-based feature selection enhances fMRI brain activity classification, [in:] *2008 5th IEEE International Symposium on Biomedical Imaging: From Nano to Macro*, Paris, France, pp. 592–595, 2008, doi: 10.1109/ISBI.2008.4541065.

17. M. Yang, K. Kpalma, J. Ronsin, A survey of shape feature extraction techniques, [in:] *Pattern Recognition Techniques, Technology and Applications*, P.Y. Yin [Ed.], I-Tech, Vienna, Austria, pp. 43–90, 2008, doi: 10.5772/6237.

18. A. Eklund, M. Andersson, H. Knutsson, fMRI analysis on the GPU—Possibilities and challenges, *Computer Methods and Programs in Biomedicine*, **105**(2): 145–161, 2012, doi: 10.1016/j.cmpb.2011.07.007.

19. S.M. Smith, A. Hyvärinen, G. Varoquaux, K.L. Miller, C.F. Beckmann, Group-PCA for very large fMRI datasets, *NeuroImage*, **101**: 738–749, 2014, doi: 10.1016/j.neuroimage.2014.07.051.

20. X. Ma, C.A. Chou, H. Sayama, W.A. Chaovalitwongse, Brain response pattern identification of fMRI data using a particle swarm optimization-based approach, *Brain Informatics*, **3**(3): 181–192, 2016, doi: 10.1007/s40708-016-0049-z.

21. H. Shahamat, A.A. Pouyan, Feature selection using genetic algorithm for classification of schizophrenia using fMRI data, *Journal of AI and Data Mining*, **3**(1): 30–37, 2015, doi: 10.5829/idosi.JAIDM.2015.03.01.04.

22. K.O. Gupta, P.N. Chatur, Cognitive state classification using genetic algorithm based linear collaborative discriminant regression, [in:] *2018 First International Conference on Secure Cyber Computing and Communication*, Jalandhar, India, pp. 180–183, 2018, doi: 10.1109/ICSCCC.2018.8703280.

23. M. Fan, C.A. Chou, Exploring stability-based voxel selection methods in MVPA using cognitive neuroimaging data: A comprehensive study, *Brain Informatics*, **3**: 193–203, 2016, doi: 10.1007/s40708-016-0048-0.

24. A. Ranjan, V.P. Singh, A.K. Singh, A.K. Thakur, R.B. Mishra, Classifying brain state in sentence polarity exposure: An ANN model for fMRI data, *Revue d'Intelligence Artificielle*, **34**(3): 361–368, 2020, doi: 10.18280/ria.340315.

25. Y. Shi, W. Zeng, N. Wang, L. Zhao, A new constrained spatiotemporal ICA method based on multi-objective optimization for fMRI data analysis, *IEEE Transactions on Neural Systems and Rehabilitation Engineering*, **26**(9): 1690–1699, 2018, doi: 10.1109/TNSRE.2018.2857501.

26. A.W. Thomas, K.R. Müller, W. Samek, Deep transfer learning for whole-brain fMRI analyses, [in:] *OR 2.0 Context-Aware Operating Theaters and Machine Learning in Clinical Neuroimaging. Lecture Notes in Computer Science*, L. Zhou *et al.* [Eds.], Vol. 11796, pp. 59–67, Springer, Cham, 2019, doi: 10.1007/978-3-030-32695-1_7.

27. M. Salehi, A. Karbasi, D.S. Barron, D. Scheinost, R.T. Constable, Individualized functional networks reconfigure with cognitive state, *NeuroImage*, **206**: 116233, 2020, doi: 10.1016/j.neuroimage.2019.116233.

28. K.H. Madsen, L.G. Krohne, X.L. Cai, Y. Wang, R.C. Chan, Perspectives on machine learning for classification of schizotypy using fMRI data, *Schizophrenia Bulletin*, **44**(suppl_ 2): S480–S490, 2018, doi: 10.1093/schbul/sby026.

29. Y. Lin *et al.*, Learning dynamic graph embeddings for accurate detection of cognitive state changes in functional brain networks, *NeuroImage*, **230**: 117791, 2021, doi: 10.1016/j.neuroimage.2021.117791.

30. Y. Zhang, L. Tetrel, B. Thirion, P. Bellec, Functional annotation of human cognitive states using deep graph convolution, *NeuroImage*, **231**: 117847, 2021, doi: 10.1016/j.neuroimage.2021.117847.

31. StarPlus fMRI data, 2001, http://www.cs.cmu.edu/afs/cs.cmu.edu/project/theo-81/www/.

32. J.S. Ramakrishna, H. Ramasangu, Cognitive state classification using clustering-classifier hybrid method, [in:] *2016 International Conference on Advances in Computing, Communications and Informatics (ICACCI)*, Jaipur, India, pp. 1880–1885, 2016, doi: 10.1109/ICACCI.2016.7732324.

33. J.S. Ramakrishna, H. Ramasangu, Classification of cognitive state using statistics of split time series, [in:] 2016 IEEE Annual India Conference (INDICON), Bangalore, India, pp. 1–5, 2016, doi: 10.1109/INDICON.2016.7839078.

Received December 27, 2021; revised version April 26, 2022;
accepted May 15, 2022; published online April 8, 2024.